Bull. Chem. Soc. Jpn., 73, 2317—2323 (2000)

Oxygen Atom Exchange Reaction between Tetradentate Schiff Base–Oxovanadium(IV) Complexes and Water

Masanobu Tsuchimoto,* Gakuse Hoshina, Ryushi Uemura, Kiyohiko Nakajima,† Masaaki Kojima,†† and Shigeru Ohba

Department of Chemistry, Faculty of Science and Technology, Keio University, Hiyoshi 3-14-1, Kohoku-ku, Yokohama 223-8522

†Department of Chemistry, Aichi University of Education, Igaya, Kariya 448-8542

††Department of Chemistry, Faculty of Science, Okayama University, Tsushima, Okayama 700-8530

(Received May 22, 2000)

The oxygen atom exchange reaction between the terminal oxygen atom (V=O) of tetradentate Schiff base–oxovanadium(IV) complexes and water slowly proceeds in DMSO solutions. The rate constants k_{obs} for the isotopic oxygen atom exchange reaction in DMSO solutions containing excess $H_2{}^{18}O$ at 50 °C under an argon atmosphere were obtained for several complexes (6×10^{-7} to 6×10^{-5} s^{-1}). The reaction proceeds faster for those complexes with electron-withdrawing groups at the Schiff base ligand moieties, and slower for the complexes with bulky hydrophobic groups. The oxygen atom exchange reaction and isomerization reaction under an argon atmosphere and in air were investigated for oxovanadium(IV) complexes that have two geometrical isomers. Water molecules attack the vanadium atom mainly from the same side of the oxo ligand for the oxovanadium(IV) complexes, whereas mainly from the opposite side of the oxo ligand for the oxovanadium(V) complexes produced by oxidation with air.

The solution chemistry of oxovanadium complexes attract the interest of many researchers these days because of their catalytic properties[1—3] and biological relevance.[4] The isomerization reaction of two diastereomeric isomers of tetradentate Schiff base–oxovanadium(IV) complexes in acetonitrile–water (95 : 5 v/v) solutions in air has been reported.[5] The isomers arising from the mutual disposition of the oxo ligand and the substituents (X) at the ligand isomerize to each other via three processes: (1) air oxidation of a fraction of the oxovanadium(IV) molecules in a solution to oxovanadium(V); (2) an oxygen atom exchange reaction between the oxovanadium(V) species and water; (3) a redox reaction between the oxovanadium(V) species and the oxovanadium(IV) molecules (Fig. 1 (a)). In process (2), water attacks the vanadium atom from the opposite side of the oxo ligand to cause isomerization (Fig. 1 (b)). However, recently we have found that the isotopic oxygen atom exchange reaction between oxovanadium(IV) complexes and $H_2{}^{18}O$ slowly proceeds even under an argon atmosphere in DMSO solutions. This result does not seem to coincide with the previous report at first glance. In this study, the rate constants k_{obs} for the isotopic oxygen atom exchange reaction in DMSO solutions containing excess $H_2{}^{18}O$ under an argon atmosphere were obtained for several oxovanadium(IV) complexes. The mechanisms of the exchange reaction for the oxovanadium(IV) complexes under an argon atmosphere and that in air are also discussed. The complexes studied in this paper are listed in Fig. 2: [VO(Xsalen)] (H_2(Xsalen): *N,N'*-di-Xsalicylidene-1,2-ethanediamine; X = H (none), 3-EtO (ethoxy), 3-*t*-Bu (*t*-butyl), 5-MeO (methoxy), 5-Cl, and 5-Br), *exo*- and *endo*-[VO(3-EtOsal-*meso*-stien)] (H_2(3-EtOsal-*meso*-stien): *N,N'*-di-3-ethoxysalicylidene-(*R,S*)(*S,R*)-1,2-diphenyl-1,2-ethanediamine), *exo*-[VO(sal-*meso*-bn)] (H_2(sal-*meso*-bn): *N,N'*-disalicylidene-(*R,S*)(*S,R*)-2,3-butanediamine), *exo*-[VO{sal-(*R*)-pn}(L)] (H_2{sal-(*R*)-pn}: *N,N'*-disalicylidene-(*R*)-1,2-propanediamine; L = H_2O, py (pyridine)), [VO(saltn)] (H_2(saltn): *N,N'*-disalicylidene-1,3-propanediamine), [VO(tpp)] (H_2tpp: tetraphenylporphin), and [VO(salen)(H_2O)]NO_3.

Experimental

Preparation of the Complexes. [VO(Xsalen)] (X = H, 3-EtO, 3-*t*-Bu, 5-MeO, 5-Cl, 5-Br),[6,7] *exo*- and *endo*-[VO(3-EtOsal-*meso*-stien)],[8,9] *exo*-[VO(sal-*meso*-bn)],[10] [VO(saltn)],[11] [VO(tpp)],[12] and [VO(salen)(H_2O)]NO_3[13,14] were prepared by the literature methods.

***exo*-[VO{sal-(*R*)-pn}(L)] (L = H_2O, py (pyridine)).** The ligand H_2{sal-(*R*)-pn} was prepared by the reaction of (*R*)-1,2-propanediamine with two equivalent amounts of salicylaldehyde in ethanol. The reaction mixture was evaporated to yield an oily product, which was used for the following reaction without purification. To a methanol solution (50 cm^3) of the ligand (20 mmol) and pyridine (10 cm^3) was added a hot methanol solution (200 cm^3) of vanadium(IV) oxide sulfate hydrate (5.0 g, 20 mmol). The reaction mixture was stirred for 30 min at 60 °C, and evaporated to yield an oily green residue. After the residue was dissolved in hot ethanol (50 cm^3), water (150 cm^3) was slowly added to the solution. After stirring for 30 min, the resulting powdered product was

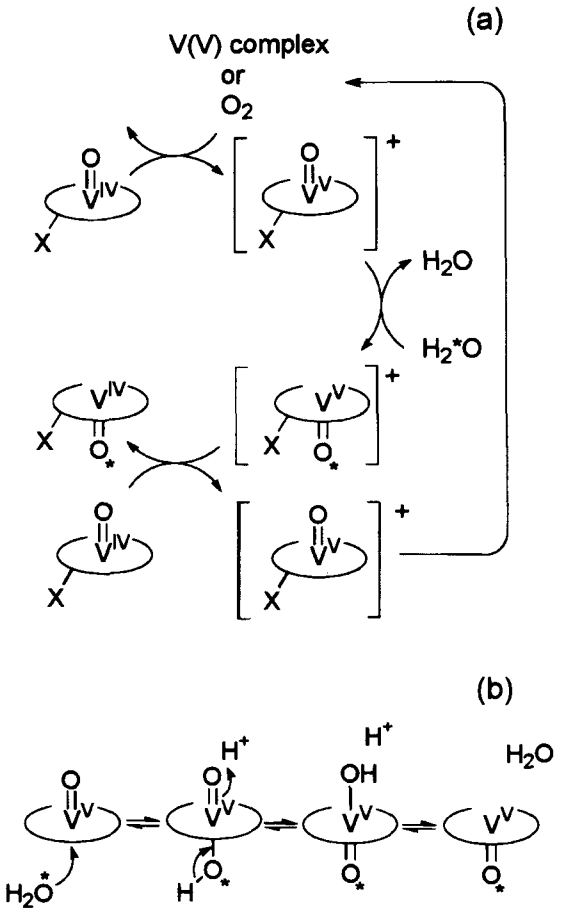

Fig. 1. Proposed mechanism for (a) the isomerization reaction of Schiff base–oxovanadium(IV) complexes in air and (b) the oxygen atom exchange reaction between Schiff base–oxovanadium(V) complexes and water.[5]

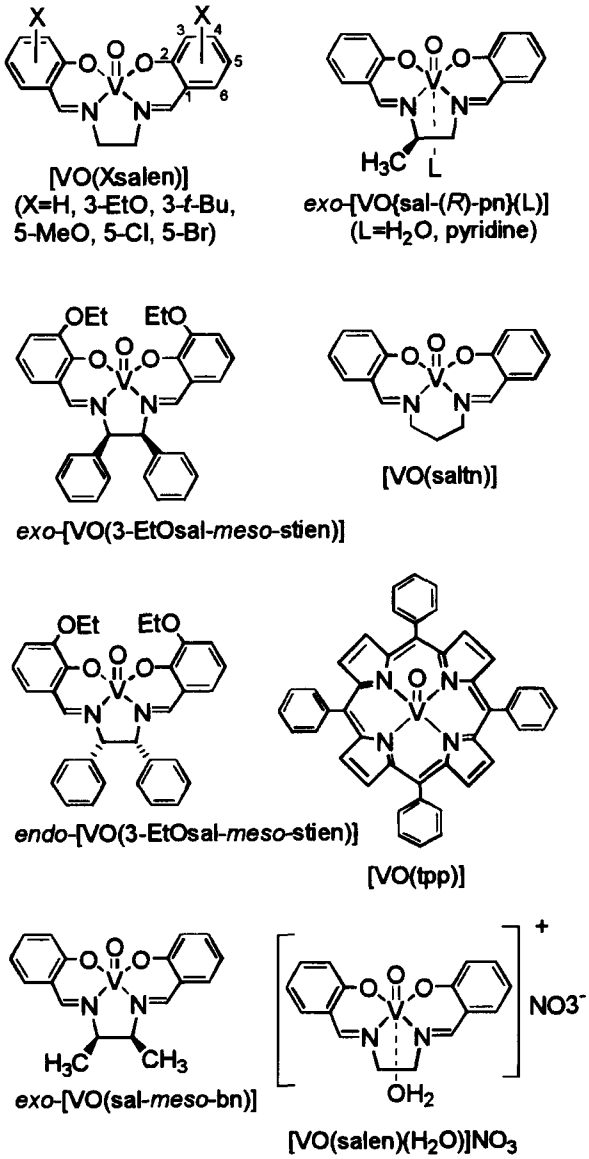

Fig. 2. Oxovanadium(IV) and oxovanadium(V) complexes studied in this paper.

collected by filtration, washed with water and dried under reduced pressure. This crude product was dissolved in dichloromethane, and an undissolved part was removed by filtration. The filtrate was evaporated to yield an oily green residue, which was recrystallized from acetonitrile and water. A mixture of green and purple powders was collected by filtration and dried. Yield: 5.1 g (74%). A high-performance liquid chromatography (HPLC) measurement showed that the mixture contained the two isomers (*exo* : *endo* ≈ 1 : 1). The mixture (3.47 g, 10 mmol) was suspended in CH_3CN–H_2O (1 : 1 (v/v), 200 cm^3) for three days in air with stirring. The color of the powder gradually turned purple. The purple powder was collected by filtration, and dried in air. The HPLC measurement showed that the purple complex contained almost exclusively one of the isomers (*exo* isomer > 95%). Yield of *exo*-[VO{sal-(*R*)-pn}(H_2O)]: 3.45 g (94%). Found: C, 55.91; H, 4.82; N, 7.60%. Calcd for $C_{17}H_{21}N_3O_3V_1$: C, 55.90; H, 4.97; N, 7.67%. UV-vis {DMSO, $\sigma/10^{-3}$ cm^{-1} ($\log \epsilon/M^{-1}$ cm^{-1})}: 15.4 (sh), 17.2 (2.21), 21.1(sh), 27.5 (3.94), 34.8 (sh), 38.3 (4.34). The dark pink *exo*-[VO{sal-(*R*)-pn}(py)] was obtained by recrystallization of *exo*-[VO{sal-(*R*)-pn}(H_2O)] (0.48 g, 1.3 mmol) from hot pyridine (3 cm^3). Yield: 0.19 g (31%). Found: C, 61.74; H, 4.88; N, 9.97%. Calcd for $C_{22}H_{21}N_3O_3V_1$: C, 61.97; H, 4.96; N, 9.86%. UV-vis {DMSO, $\sigma/10^{-3}$ cm^{-1} ($\log \epsilon/M^{-1}$ cm^{-1})}: 15.5 (sh), 17.2 (2.16), 21.1(sh), 27.5 (3.97), 34.7 (sh), 38.3 (4.40).

Thermal Analysis. A thermogravimetry (TG) measurement of *exo*-[VO{sal-(*R*)-pn}(H_2O)] up to 100 °C was carried out with a heating rate of 5 °C min^{-1} on a Rigaku Thermoplus TG 8120 thermal analyzer. The measurement showed a 4.15% weight loss between 30—60 °C, which corresponds to 0.84 mol of water per vanadium complex.

Kinetic Measurements. All the organic solvents were dried and degassed prior to use, and treated under an argon atmosphere. To a DMSO solution (25 cm^3) of the complex (0.05 mmol) was added 0.1 cm^3 (ca. 5 mmol) of $H_2{}^{18}O$ (> 95 atom%) and the solution was kept at 50 °C under an argon atmosphere. Approximately 2 cm^3 portions of the solution were taken out from the vessel at regular time intervals, and immediately evaporated to dryness below 40 °C under reduced pressure.[15] The IR spectra of the products were measured in KBr disks. The rate constants k_{obs} were evaluated from the least-squares slopes of the graph of ln ([a]/([a]−[x])) vs. time, where [a] is the initial concentration of [$V^{16}O$(L)] (L: Schiff base), and [x] is the concentration of [$V^{18}O$(L)] produced. The [a]/([a]−[x]) values were evaluated from the absorption band areas of the V = ^{16}O and V = ^{18}O stretching bands. The plot of

ln([a]/([a]−[x])) vs. time gave a straight line for at least a half life.[16] The rate constants in acetonitrile solution under an argon atmosphere were obtained by a similar method.

Crystal Structure Determination. Pink prismatic crystals of *exo*-[VO{sal-(*R*)-pn}(py)] were obtained by slow diffusion of diethyl ether vapor into a pyridine solution of *exo*-[VO{sal-(*R*)-pn}(H_2O)]. Green prismatic crystals of [VO(3-*t*-Busalen)] were grown from an acetonitrile solution. The intensity data were collected at 25 °C on a Rigaku four-circle AFC-7R diffractometer with graphite-monochromatized Mo $K\alpha$ radiation (λ = 0.71073 Å) up to 2θ = 55° by θ—2θ scans. Three standard reflections were measured at every 150 reflections. Absorption corrections were made by the Ψ scans method.[17] The structures were solved by direct methods on a Silicon Graphics O^2 workstation with the program system TEXSAN.[18] Non-hydrogen atoms were treated anisotropically, and hydrogen atoms attached to carbon atoms were introduced at ideal positions. The refinement was based on F against all the 2643 reflections for *exo*-[VO{sal-(*R*)-pn}(py)], and against all the 5324 reflections for [VO(3-*t*-Busalen)]. The absolute structure of *exo*-[VO{sal-(*R*)-pn}(py)] was assigned on the basis of the known configuration of (*R*)-1,2-propanediamine, and was confirmed by the Flack parameter, $x = -0.02(5)$.[19] The crystal data and experimental details are listed in Table 1. Crystallographic data have been deposited at the CCDC, 12 Union Road, Cambridge CB2 1EZ, UK and copies can be obtained on request, free of charge, by quoting the publication citation and the deposition numbers CCDC 147289 and 147290. The complete data are deposited as Document No. 73058 at the Office of the Editor of Bull. Chem. Soc. Jpn.

Measurements. IR spectra were recorded on a JASCO A-202 spectrophotometer. KBr disks (3 mm ϕ) were prepared with a JASCO MP-1 disk modeling kit and a JASCO MT-1 press. Electronic spectra were recorded on a JASCO V-570 spectrophotometer. Cyclic voltammetric measurements were carried out using a Fuso HECS 321B potential sweep unit on DMSO solutions at 25 °C (1 mM complex, 0.1 M $N(C_4H_9)_4BF_4$) at a scan rate of 0.1 V s^{-1} (1 M = 1 mol dm^{-3}). A glassy carbon electrode, an $Ag/AgNO_3$ electrode (Ag/0.01 M $AgNO_3$), and a platinum wire were employed as the working, reference, and auxiliary electrodes, respectively. As an external standard, the F_c^+/F_c (F_c = ferrocene) couple was observed at 0.172 V vs. Ag/Ag^+ under these conditions. HPLC was carried out with a Shimadzu LC-10AD pumping unit and a Shimpack CLC-ODS column. Acetonitrile–water solutions (7 : 3 v/v for *exo*- and *endo*-[VO(3-EtOsal-*meso*-stien)], 1 : 1 v/v for *exo*-[VO(sal-*meso*-bn)], 45 : 55 v/v for *exo*-[VO{sal-(*R*)-pn}(L)]) were used as eluents. The components separated by chromatography were detected with a Shimadzu SPD-10A UV-vis detector at 250 nm.

Table 1. Crystallographic Data for [VO{sal-(*R*)-pn}(py)] and [VO(3-*t*-Busalen)]

	[VO{sal-(*R*)-pn}(py)]	[VO(3-*t*-Busalen)]
Chemical formula	$C_{22}H_{21}N_3O_3V$	$C_{24}H_{30}N_2O_3V$
fw	426.4	445.5
Crystal size/mm	0.50×0.47×0.15	0.45×0.40×0.20
Space group	$P2_12_12_1$	$P\bar{1}$
a/Å	16.951(3)	12.636(3)
b/Å	18.155(3)	12.901(4)
c/Å	6.499(4)	7.697(2)
α/°	90	100.85(2)
β/°	90	95.99(2)
γ/°	90	106.88(2)
V/Å^3	2000(1)	1162.2(5)
Z	4	2
ρ_{calc}/g cm^{-3}	1.416	1.273
μ/cm	5.24	4.53
λ/Å	0.71073	0.71073
Temp/°C	25	25
$R^{a)}(I > 2\sigma(I))$	0.042	0.033
$R_w{}^{b)}$	0.098	0.061

a) $R = \sum||F_o| - |F_c||/\sum|F_o|$. b) $R_w = [\sum w\ (|F_o| - |F_c|)^2/\sum w|F_o|^2]^{1/2}$, $w^{-1} = \sigma^2(|F_o|) + 0.00483|F_o|^2$ for [VO{sal-(*R*)-pn}(py)], and $w^{-1} = \sigma^2(|F_o|) + 0.00164|F_o|^2$ for [VO(3-*t*-Busalen)].

Results and Discussion

Synthesis. The oxovanadium(IV) complex with the ligand sal-(*R*)-pn can have two geometrical isomers (*exo*- and *endo*-isomers)[8] arising from the mutual disposition of the oxo ligand and the methyl group. One of the isomers, *exo*-[VO{sal-(*R*)-pn}(L)] (L = H_2O, py), was isolated. The reaction of the Schiff base ligand with vanadium(IV) oxide sulfate in methanol gave a mixture of green and purple powder. The HPLC measurement showed that the mixture contained the two isomers (*exo* : *endo* ≈ 1 : 1). Upon suspending in a CH_3CN–H_2O (1 : 1 (v/v)) solution in air for three days, the mixture gradually turned into a purple powder. The HPLC measurement showed that the purple complex was almost exclusively one of the isomers (> 95%). The IR spectrum of the purple complex shows a V=O stretching band at 975 cm^{-1}. The purple powder changed to a green powder (ν(V=O): 981 cm^{-1}) when it was dried under reduced pressure or upon heating at 60 °C. However, the purple powder was regenerated in a few minutes when the green powder was exposed to air. The IR, TG, and elemental analytical data suggest that the purple complex is [VO{sal-(*R*)-pn}(H_2O)], which has a water ligand *trans* to the oxo ligand. The water molecule weakly bonded to the vanadium atom will be removed under reduced pressure or upon heating to yield green [VO{sal-(*R*)-pn}]. Recrystallization of the complex from pyridine gave dark-pink *exo*-[VO{sal-(*R*)-pn}(py)], whose structure was confirmed by an X-ray crystal structure analysis. The progress of the isomerization from the *endo*- to the *exo*-isomer during the process of suspending the mixture in a CH_3CN–H_2O solution could be due to both the lower solubility of the *exo*-isomer than that of the *endo*-isomer, and the conditions in which the isomerization reaction can occur (vide infra).

X-Ray Crystal Structures. X-Ray crystal structure analyses of *exo*-[VO{sal-(*R*)-pn}(py)] and [VO(3-*t*-Busalen)] were carried out. Molecular structures are shown in Figs. 3 and 4. Selected bond lengths and angles are listed in Tables 2 and 3. The geometry around the vanadium atom of *exo*-[VO{sal-(*R*)-pn}(py)] is a distorted octahedron with a weak coordination of a pyridine molecule (V1–N7 distance: 2.636(5) Å) in the position *trans* to the oxo ligand. The V=O distance is 1.589(4) Å, and the V1 atom is displaced by 0.370(2) Å from the equatorial N_2O_2 coordination plane. The five-membered N–N chelate ring takes a distorted gauche conformation with the methyl group in the axial position on

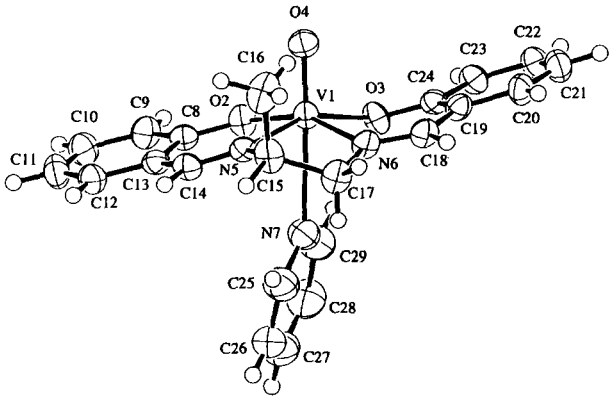

Fig. 3. ORTEP drawing of [VO{sal-(*R*)-pn}(py)] with 50% probability ellipsoids.

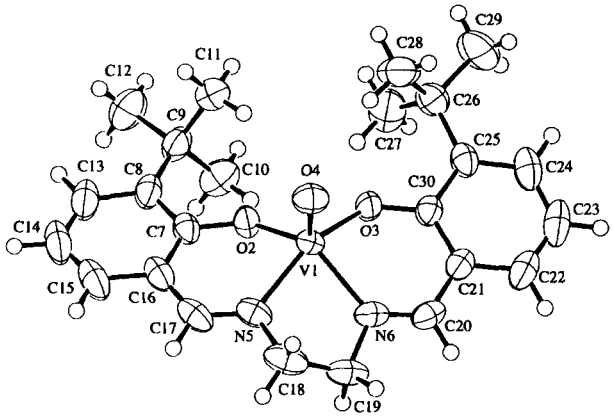

Fig. 4. ORTEP drawing of [VO(3-*t*-Busalen)] with 50% probability ellipsoids.

Table 2. Selected Bond Lengths (*l*/Å) and Angles (ϕ/deg) of [VO{sal-(*R*)-pn}(py)]

V1–O2	1.947(3)	V1–O3	1.947(3)
V1–O4	1.589(4)	V1–N5	2.062(4)
V1–N6	2.063(4)	V1–N7	2.636(5)
O2–V1–O3	95.2(1)	O2–V1–O4	102.3(2)
O2–V1–N5	89.7(1)	O2–V1–N6	158.2(2)
O2–V1–N7	76.4(2)	O3–V1–O4	102.0(2)
O3–V1–N5	156.2(2)	O3–V1–N6	87.8(1)
O3–V1–N7	80.8(1)	O4–V1–N5	99.6(2)
O4–V1–N6	98.2(2)	O4–V1–N7	177.0(2)
N5–V1–N6	79.4(2)	N5–V1–N7	77.7(2)
N6–V1–N7	82.8(2)		

the same side of the oxo ligand (*exo*-isomer).

The geometry around the vanadium atom of [VO(3-*t*-Busalen)] is a distorted square-pyramidal structure with the oxo ligand (O4) in the apical position. The V=O distance is 1.596(1) Å, and the V1 atom is displaced by 0.6367(7) Å from the equatorial N_2O_2 coordination plane. The C9 and C26 atoms of the *t*-butyl substituents at the 3-positions deviate from the equatorial N_2O_2 plane in the axial positions opposite to each other (−0.495(3) Å for C9 and + 0.670(3) Å for C26) to reduce the steric repulsion between the *t*-butyl groups.

Table 3. Selected Bond Lengths (*l*/Å) and Angles (ϕ/deg) of [VO(3-*t*-Busalen)]

V1–O2	1.912(1)	V1–O3	1.933(1)
V1–O4	1.596(1)	V1–N5	2.051(1)
V1–N6	2.062(1)		
O2–V1–O3	87.94(4)	O2–V1–O4	113.51(6)
O2–V1–N5	86.13(5)	O2–V1–N6	134.12(5)
O3–V1–O4	105.63(6)	O3–V1–N5	151.39(6)
O3–V1–N6	86.37(5)	O4–V1–N5	102.40(6)
O4–V1–N6	111.85(6)	N5–V1–N6	77.94(6)

Oxygen Atom Exchange Reaction. The oxygen atom exchange reaction between the terminal oxygen atom (V=O) of the Schiff base-oxovanadium(IV) complexes and water slowly proceeds in DMSO solutions. The rate constants k_{obs} for the isotopic oxygen atom exchange reaction in DMSO solutions containing a large excess of $H_2{}^{18}O$ at 50 °C under an argon atmosphere were evaluated using IR data. Table 4 lists the k_{obs} data, the V=^{16}O and V=^{18}O stretching frequencies,[20] and V(V)/V(IV) redox potentials. The k_{obs} values (k_{obs} = $6\times10^{-7}-6\times10^{-5}$ s^{-1} at 50 °C) for the present study are smaller than that for $[VO(H_2O)_5]$ (k_{obs} = $(2.98\pm0.25)\times10^{-5}$ s^{-1}, in H_2O at 0 °C.[21] For [VO(Xsalen)] (X=H, 3-EtO, 5-MeO, 5-Cl, 5-Br), the reaction rates of the complexes that have electron-withdrawing groups and positive $E_{1/2}$ values (k_{obs} = 6×10^{-5} s^{-1} and $E_{1/2}$ = 0.166 V for [VO(5-Br-salen)], k_{obs} = 4×10^{-5} s^{-1} and $E_{1/2}$ = 0.162 V for [VO(5-Clsalen)]) are faster than those of the other complexes (k_{obs} = $1\times10^{-5}-2\times10^{-5}$ s^{-1} and $E_{1/2}$ = 0.017 − 0.071 V). An increase in the positive charge on the vanadium atom could accelerate the exchange reaction. On the other hand, the reactions proceed more slowly for the complexes with bulky hydrophobic groups (k_{obs} = 6×10^{-6} s^{-1} for [VO(3-*t*-Busalen)], 6×10^{-7} s^{-1} for *exo*-[VO(3-EtOsal-*meso*-stien)], and 4×10^{-6} s^{-1} for *endo*-[VO(3-EtOsal-*meso*-stien)]). Figures 4 and 5 show structures of [VO(3-*t*-Busalen)] and *exo*- and *endo*-[VO(3-EtOsal-*meso*-stien)]. The hydrophobic *t*-butyl or phenyl groups are oriented in the axial positions in these complexes. Water molecules would have difficulty in approaching the vanadium atom of these complexes in solutions. The exchange reaction did not occur for [VO(tpp)], whose vanadium atom is surrounded by the hydrophobic macrocyclic ligand. For [VO(saltn)], which has a polymeric linear chain structure (···V=O···V=O···) in the solid state and a distorted octahedral structure with weak coordination of a solvent molecule in DMSO solution,[7] the exchange reaction was completed within two days. However, the rate constant could not be obtained because of a poor separation of the V=^{16}O and V=^{18}O stretching bands. The reaction of the oxovanadium(V) complex [VO(salen)-(H_2O)]NO_3 (k_{obs} = 3×10^{-4} s^{-1} in CH_3CN at 25 °C) proceeds much faster than those of the other oxovanadium(IV) complexes.

The reaction rates in acetonitrile solutions were obtained

Table 4. IR Data, Kinetic Data and Redox Potentials for the V(V)/V(IV) Couples of Oxovanadium(IV) and (V) Complexes

Complex	$\nu(V=^{16}O)/cm^{-1}$	$\nu(V=^{18}O)/cm^{-1}$	k_{obs}/s^{-1} [a]	$E_{1/2}/V(\Delta E_p/mV)$ [b]
[VO(salen)]	981,988	941,946	1×10^{-5}	0.071(75)
			2×10^{-5} [c]	
[VO(3-EtOsalen)]	979	940	1×10^{-5}	0.032(73)
			2×10^{-5} [c]	
[VO(5-MeOsalen)]	976,988	937	2×10^{-5}	0.017(77)
			4×10^{-5} [c]	
[VO(5-Clsalen)]	964,990	943	4×10^{-5}	0.162(76)
[VO(5-Brsalen)]	990	943	6×10^{-5}	0.166(79)
[VO(3-*t*-Busalen)]	985	931	6×10^{-6}	−0.063(75)
exo-[VO(3-EtOsal-*meso*-stien)]	977,987	939	6×10^{-7}	0.095(80)
endo-[VO(3-EtOsal-*meso*-stien)]	988	944	4×10^{-6}	0.168(66)
exo-[VO(sal-*meso*-bn)]	987	947	1×10^{-6}	0.050(73)
exo-[VO{sal-(*R*)-pn}(H_2O)]	966	927	1×10^{-5}	0.076(73)
exo-[VO{sal-(*R*)-pn}(py)]	955[d]	—[e]	5×10^{-6}	0.071(76)
[VO(saltn)]	859	826	—[f]	0.219(70)
[VO(tpp)]	1005	—[g]	—[g]	—[h]
[VO(salen)(H_2O)]NO_3	965,975	925	3×10^{-4} [i]	

a) In a DMSO solution at 50 °C unless otherwise noted. b) All the $E_{1/2}$ values are given vs. Ag/Ag^+. $E_{1/2}$ is calculated as the average of anodic (E_{pa}) and cathodic (E_{pc}) potentials; $\Delta E_p = E_{pa} - E_{pc}$. c) In an acetonitrile solution at 50 °C. d) By a Nujol mull method. e) Upon evaporation of a reaction mixture of *exo*-[VO{sal-(*R*)-pn}(py)] and $H_2{}^{18}O$ in DMSO under reduced pressure, *exo*-[$V^{18}O${sal-(*R*)-pn}(H_2O)] was obtained. f) The rate constant could not be obtained because of a poor separation of the $V=^{16}O$ and $V=^{18}O$ stretching bands. g) The exchange reaction did not occur. h) The V(V)/V(IV) couple was not observed. i) In an acetonitrile solution at 25 °C.

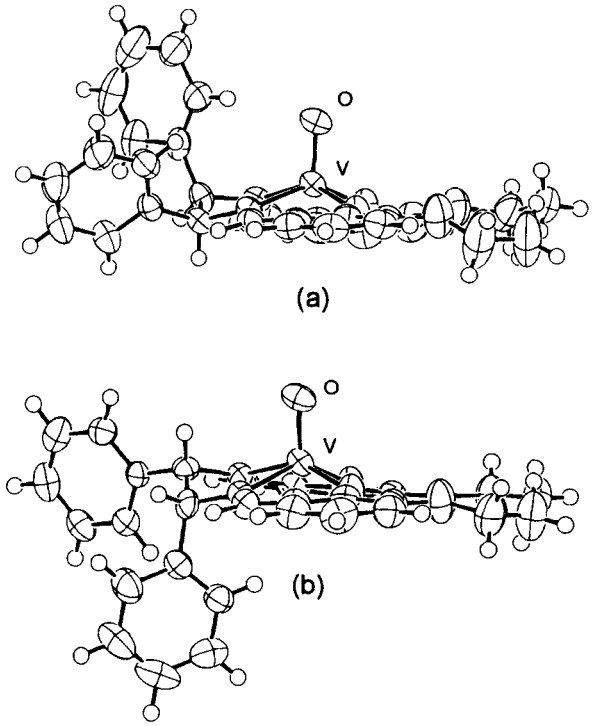

Fig. 5. Side views of (a) *exo*-[VO(3-EtOsal-*meso*-stien)] and (b) *endo*-[VO(3-EtOsal-*meso*-stien)].[8,9]

for [VO(Xsalen)] (X = H, 3-EtO, and 5-MeO). There is not much difference between the rates in DMSO and those in acetonitrile. However, the exchange reaction proceeds rapidly in a weakly acidic solvent. The reaction of [VO(salen)] with $H_2{}^{18}O$ in acetic acid at 50 °C was too fast to be followed and was completed within 30 min. The rate constants could not be obtained in basic pyridine solutions because of the slow decomposition of the complexes.

To examine the mechanism of the exchange reaction, the relationship between the oxygen atom exchange reaction and the isomerization reaction was investigated for those oxovanadium(IV) complexes having two geometrical isomers. Table 5 shows the degree of isomerization in the exchange reaction under an argon atmosphere. Table 6 shows the isomer ratio at equilibrium and the time required to attain equilibrium in the reaction in air. Under an argon atmosphere, the oxygen atom exchange reaction proceeded slowly with little progress of the isomerization. On the other hand, the isomerization reaction proceeded rapidly in air and attained equilibrium within a few hours except for [VO(sal-*meso*-bn)].[22] These results suggest that the mechanism of the oxygen atom exchange reaction under an argon atmo-

Table 5. Isomer Ratio[a] at the Time When the Exchange Reaction Proceeded to 50%[b] under an Argon Atmosphere.[c]

Complex	Isomer ratio / %	$t_{1/2}$ / h[d]
exo-[VO(3-EtOsal-*meso*-stien)]	5.4	320
endo-[VO(3-EtOsal-*meso*-stien)]	99	48
exo-[VO(sal-*meso*-bn)]	6.0	192
exo-[VO{sal-(*R*)-pn}(H_2O)]	9.3	19
exo-[VO{sal-(*R*)-pn}(py)]	9.0	38

a) ([*endo*]/[*exo*]+[*endo*])×100. b) ([^{18}O]/[^{18}O]+[^{16}O]) ×100. c) In a DMSO solution containing 2 mM of the complex and 0.2 M of $H_2{}^{18}O$ at 50 °C. d) The half-life of the oxygen atom exchange reaction.

Table 6. Isomer Ratio[a] at Equilibrium and the Time Required to Attain Equilibrium for the Reaction in Air[b]

Complex	Isomer ratio	Time
	%	h
exo-[VO(3-EtOsal-*meso*-stien)]	77	3
endo-[VO(3-EtOsal-*meso*-stien)]	77	0.5
exo-[VO(sal-*meso*-bn)]	54	48
exo-[VO{sal-(*R*)-pn}(H_2O)]	49	1
exo-[VO{sal-(*R*)-pn}(py)]	48	1.5

a) ([*endo*]/[*exo*]+[*endo*])×100. b) In a DMSO solution containing 2 mM of the complex and 0.2 M of H_2O at 50 °C.

sphere is different from that in air. Water molecules will attack the vanadium atom mainly from the same side of the oxo ligand for the oxovanadium(IV) complexes (Fig. 6), whereas mainly from the opposite side of the oxo ligand for the oxovanadium(V) complexes produced by oxidation with air (Fig. 1(b)). As water molecules attack the vanadium atom mainly from the same side of the oxo ligand, isomerization scarcely proceeds in the reaction under an argon atmosphere. The slower exchange reaction of *exo*-[VO(3-EtOsal-*meso*-stien)] ($k_{obs} = 6\times10^{-7}$ s^{-1}) than that of *endo*-[VO(3-EtOsal-*meso*-stien)] ($k_{obs} = 4\times10^{-6}$ s^{-1}) under an argon atmosphere is in accord with the mechanism. The *exo*-isomer has an axially-oriented hydrophobic phenyl substituent on the same side of the oxo ligand, whereas the *endo*-isomer has the substituent on the opposite side of the oxo ligand (Fig. 5).

The difference between the reaction mechanism for the oxovanadium(IV) complexes and that for the oxovanadium(V) complexes can be explained based on the difference in their structures. Most tetradentate Schiff base–oxovanadium(IV) complexes have five-coordinate monomeric structures with a square-pyramidal geometry, and several oxovanadium(IV) complexes have six-coordinate polymeric linear chain structures (···V=O···V=O···)[11] or monomeric distorted octahedral structures with weak coordination of a solvent molecule in the position trans to the oxo ligand.[23] On the other hand, all Schiff base–oxovanadium(V) complexes have six-coordinate octahedral structures with weak coordination of a solvent molecule[13,24] or a counter anion.[25,26] In other words, oxovanadium(IV) complexes tend to have a square-pyramidal structure, whereas oxovanadium(V) complexes tend to have an octahedral structure. The deviation of the vanadium atom from the N_2O_2 coordination plane is usually 0.50—0.63 Å for the Schiff base–oxovanadium(IV) complexes with square-pyramidal structures,[7–10,27,28] 0.27—0.40 Å for the Schiff base–oxovanadium(IV) complexes with octahedral structures (polymeric and monomeric complexes),[11,23,28,29] and 0.21—0.32 Å for the Schiff base-oxovanadium(V) complexes with octahedral structures.[13,24–26] The DMSO solutions of all the oxovanadium (IV) complexes in Table 5 are green, and their electronic spectra show d–d transition bands characteristic of the complexes with square-pyramidal structures.[6,7,9,10] The large deviation will cause an attack of water molecules on the vanadium atom from the same side of the oxo ligand to be more favorable.

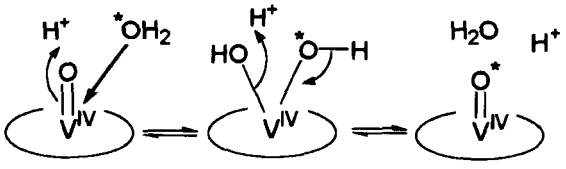

Fig. 6. Proposed mechanism for the oxygen atom exchange reaction between oxovanadium(IV) complexes and water.

Small progress of the isomerization reaction (< 10%) was observed in the reaction under an argon atmosphere, as shown in Table 5. It may be due to the mechanism that a part of the water molecules attack the vanadium atom from the opposite side of the oxo ligand. Although most water molecules in the solution are supposed to attack the vanadium atom from the same side of the oxo ligand, there may be a small amount of the molecules that attack the vanadium atom from the opposite side of the oxo ligand, especially for *exo*-[VO{sal-(*R*)-pn}(L)] (L = H_2O, py), which tend to form distorted octahedral structures in the solid state.

The authors thank Mr. Hidenori Fushiki (Keio University) for his assistance in the kinetic measurements.

References

1 K. Yamamoto, K. Oyaizu, and E. Tsuchida, *J. Am. Chem. Soc.*, **118**, 12665 (1996).

2 E. Tsuchida, K. Oyaizu, E. L. Dewi, T. Imai, and F. C. Anson, *Inorg. Chem.*, **38**, 3704 (1999).

3 K. Nakajima, K. Kojima, M. Kojima, and J. Fujita, *Bull. Chem. Soc. Jpn.*, **63**, 2620 (1990).

4 N. D. Chateen, *Struct. Bonding (Berlin)*, **53**, 105 (1983).

5 K. Nakajima, M. Kojima, M. Tsuchimoto, Y. Yoshikawa, and J. Fujita, *Chem. Lett.*, **1994**, 1693.

6 A. Pasini and M. Gulloti, *J. Coord. Chem.*, **3**, 319 (1974).

7 M. Tsuchimoto, R. Kasahara, K. Nakajima, M. Kojima, and S. Ohba, *Polyhedron*, **18**, 3035 (1999).

8 G. Hoshina, M. Tsuchimoto, S. Ohba, K. Nakajima, H. Uekusa, Y. Ohashi, and M. Kojima, *Inorg. Chem.*, **37**, 142 (1998).

9 G. Hoshina, S. Ohba, K. Nakajima, H. Ishida, M. Kojima, and M. Tsuchimoto, *Bull. Chem. Soc. Jpn.*, **72**, 1037 (1999).

10 G. Hoshina, M. Tsuchimoto, and S. Ohba, *Acta Crystallogr., Sect. C*, **C55**, 1082 (1999).

11 M. Mathew, A. J. Carty, and G. J. Palenik, *J. Am. Chem. Soc.*, **92**, 3197 (1970).

12 E. C. Jhonson and D. Dolphin, *Inorg. Synth.*, **20**, 143 (1980).

13 M. Tsuchimoto, E. Yasuda, and S. Ohba, *Chem. Lett.*, **2000**, 562.

14 K. Nakajima, K. Kojima, M. Kojima, and J. Fujita, *Bull. Chem. Soc. Jpn.*, **63**, 2620 (1990).

15 The exchange reaction will scarcely proceed during the evaporation process, as water is removed before DMSO is evaporated.

16 As examples, the graphs of ln([a]/([a]−[x])) vs. time for [VO{sal-(*R*)-pn}(py)] and [VO(salen)]NO_3 are deposited as Document No.73058 at the Office of the Editor of Bull. Chem. Soc. Jpn.

17 A. C. T. North, D. C. Phillips, and F. S. Mathews, *Acta Crystallogr., Sect. A*, **A24**, 351 (1968).

18 "TEXSAN, Single crystal structure analysis software. Ver-

sion 1.9. MSC, 3200 Research Forest Drive," The Woodlands, TX 77381, U.S.A (1988).

19 H. D. Flack, *Acta Crystallogr., Sect A*, **A39**, 876 (1983).

20 Some complexes show two V=^{16}O stretching bands. These complexes may have two types of crystals which have different V=O stretching frequencies.

21 R. K. Murmann, *Inorg. Chim. Acta*, **25**, L43 (1977).

22 [VO(sal-*meso*-bn)] has a similar redox potential (0.050 V) to those of [VO{sal-(*R*)-pn}(L)] (L = H_2O (0.076 V), py (0.071 V)). The slow isomerization reaction of [VO(sal-*meso*-bn)] in air cannot be explained at present.

23 C. A. Root, J. D. Hoeschele, C. R. Cornman, J. W. Kampf, and V. L. Pecoraro, *Inorg. Chem.*, **32**, 3855 (1993).

24 L. Banci, A. Bencini, A. Dei, and D. Gatteschi, *Inorg. Chim. Acta.*, **84**, L11 (1984).

25 M. Tsuchimoto and S. Ohba, *Acta Crystallogr., Sect. C*, **C55**, IUC9900008 (1999).

26 J. A. Bonadies, W. M. Butler, V. L. Pecoraro, and C. J. Carrano, *Inorg. Chem.*, **26**, 1218 (1987).

27 For example: a) P. E. Riley, V. L. Pecoraro, C. J. Carrano, J. A. Bonadies, and K. N. Raymond, *Inorg. Chem.*, **25**, 154 (1986). b) M. Pasquali, F. Marchetti, C. Floriani, and M. Cesali, *Inorg. Chem.*, **19**, 1198 (1980). c) J. R. Zamian, E. R. Dockal, G. Castellano, G. Oliva, *Polyhedron*, **14**, 2411 (1995).

28 a) R. Kasahara, M. Tsuchimoto, S. Ohba, K. Nakajima, H. Ishida, and M. Kojima, *Inorg. Chem.*, **35**, 7661 (1996). b) K. Nakajima, M. Kojima, S. Azuma, R. Kasahara, M. Tsuchimoto, Y. Kubozono, H. Maeda, S. Kashino, S. Ohba, Y. Yoshikawa, and J. Fujita, *Bull. Chem. Soc. Jpn.*, **69**, 3207 (1996).

29 a) S. A. Fairhurst, D. L. Hughes, U. Kleinkes, G. J. Leigh, J. R. Sanders, and J. Weisner, *J. Chem. Soc., Dalton Trans.*, **1995**, 321. b) M. Tsuchimoto, G. Hoshina, N. Yoshioka, H. Inoue, K. Nakajima, M. Kamishima, M. Kojima, and S. Ohba, *J. Solid State Chem.*, **153**, 9 (2000).